Inter-Point Procrustes: Identifying Regional and Large Differences in 3D Anatomical Shapes

Karim Lekadir[1], Alejandro F. Frangi[1], and Guang-Zhong Yang[2]

[1] Center for Computational Imaging & Simulation Technologies in Biomedicine
Universitat Pompeu Fabra and CIBER-BBN, Barcelona, Spain
[2] Hamlyn Centre for Robotic Surgery, Imperial College London, United Kingdom

Abstract. This paper presents a new approach for the robust alignment and interpretation of 3D anatomical structures with large and localized shape differences. In such situations, existing techniques based on the well-known Procrustes analysis can be significantly affected due to the introduced non-Gaussian distribution of the residuals. In the proposed technique, influential points that induce large dissimilarities are identified and displaced with the aim to obtain an intermediate template with an improved distribution of the residuals. The key element of the algorithm is the use of pose invariant shape variables to robustly guide both the influential point detection and displacement steps. The intermediate template is then used as the basis for the estimation of the final pose parameters between the source and destination shapes, enabling to effectively highlight the regional differences of interest. The validation using synthetic and real datasets of different morphologies demonstrates robustness up-to 50% regional differences and potential for shape classification.

1 Introduction

Procrustes analysis is a well-established approach for the alignment and interpretation of sets of corresponding landmark shapes [1]. Statistical shape modeling [2], shape classification [3], and regional shape analysis [4] are amongst the most common applications. In medical imaging, the shape complexity and the high variability means the 3D alignment needs to be robust and consistent in order to allow for a biologically meaningful analysis. It is now accepted that the standard Procrustes with its least square minimization can introduce errors in the presence of large shape differences [3, 5]. This is particularly the case when the shape variation is localized in a region of the anatomy, thus generating a non-Gaussian distribution of the residuals in both the spatial and frequency domains. Such situation is common in medical imaging, for instance due to abnormal remodeling at specific regions of the anatomy [4]. Thus far, the most common strategy to improve the Procrustes analysis is by using robust statistics (such as by using M-estimators [6]) but the performance is limited for regional shape analysis. More recently, two approaches have been proposed to increase the robustness of the Procrustes alignment. Firstly, the method in [7] replaces the least squares criterion with the more robust L_1-norm, but the technique is only valid in 2D, while anatomical shapes are mostly studied in 3D and increasingly in 4D.

N. Ayache et al. (Eds.): MICCAI 2012, Part III, LNCS 7512, pp. 99–106, 2012.

A supervised Procrustes was also presented in [3] with the aim to aid classification, but the method requires a potentially biased or unavailable prior input.

In this paper, we propose a new Procrustes method that is unsupervised, robust and can be applied to different morphology types. To this end, instead of introducing a new similarity or minimization scheme, the proposed technique uses pose invariant shape variables to robustly compare the landmark configurations and to generate an intermediate template that is used for a geometrically meaningful alignment. More specifically, the influential landmarks (*i.e.*, those corresponding to large residuals) are identified using an invariant measure of dissimilarity and thus independently of the initial pose. Subsequently, these points are displaced within the source shape such that the new invariant discrepancies are minimized. The intermediate template as compared to the destination shape is free of large landmark residuals, thus enabling a successful final Procrustes alignment of the two input shapes. Detailed synthetic and real data experiments with various morphologies are carried out to assess the performance of the introduced algorithm and its value for shape discrimination.

2 Methods

2.1 Invariant Detection of Influential Points

The presence of regional anatomical differences means a subset of the landmarks carry a large amount of the total shape variability. Conventionally, the identification and handling of these influential points is achieved by performing an initial Procrustes alignment, followed by an iterative weighting of the landmarks based on the obtained landmark residuals. However, when the differences are large and localized, this initial least squares Procrustes becomes significantly and irreversibly corrupted, which does not allow for accurate weighting of the landmarks at subsequent iterations. To tackle this problem, we present in this work a new procedure for influential landmark identification that is independent of any pose estimation. To this end, variables that exclusively describe shape information are used. Let us denote $\mathbf{x}^{(s)}$ and $\mathbf{x}^{(d)}$ the source and destination shape vectors, respectively, encapsulating the coordinates of n corresponding points ($\mathbf{x}_i = (x_i, y_i, z_i)^T$ $(1 \le i \le n)$). For the proposed technique, each shape is associated with an inter-landmark distance matrix $\mathbf{D}$ of size $n \times n$, *i.e.*, :

$$\mathbf{D} = \begin{bmatrix} 0 & d_{12} & \dots & \dots & d_{1n} \\ d_{21} & 0 & \dots & \dots & d_{2n} \\ \dots & \dots & \dots & \dots & \dots \\ \dots & \dots & \dots & \dots & \dots \\ d_{n1} & d_{n2} & \dots & \dots & 0 \end{bmatrix} \quad (1)$$

where $d_{ij} = \left\| \mathbf{x}_i - \mathbf{x}_j \right\|_2$ is the Euclidean distance between points p_i and p_j. Such shape variables have the advantage over point coordinates to be invariant to both

translation and rotation of the shapes. Furthermore, they can be used to robustly correct for size differences, by applying to $\mathbf{x}^{(s)}$ the following robust scaling factor:

$$\underset{1\le i<j\le n}{\text{med}}\left(\frac{d_{ij}^{(d)}}{d_{ij}^{(s)}}\right). \tag{2}$$

The aim of the proposed method is to derive an invariant and robust measure of shape dissimilarity at each landmark point based on the differences in the inter-landmark distances calculated from the two shapes. Typically, a landmark associated with a significant shape difference will have many large differences of corresponding inter-landmark distances. Similarly, points corresponding to smaller shape residuals will have a large number of small inter-landmark differences. As a result, a median based measure of shape dissimilarity at each landmark is introduced as follows:

$$\delta_i = \underset{1\le j\le n}{\text{med}}\left[(d_{ij}^{(s)} - d_{ij}^{(d)})^2\right]. \tag{3}$$

δ_i gives a good indication of the type of histogram involved with the inter-landmark differences for the point p_i. Subsequently, the set A of influential points is expected to be associated with particularly high δ_i values. Based on robust statistics [8], an appropriate definition of A can be derived by using robust estimations of the average point dissimilarity and deviation, *i.e,*:

$$A = \left\{p_k \mid \delta_k > c(1.4826 \underset{1\le i\le n}{\text{med}}\left|\delta_i - \delta^*\right|)\right\} \text{ where } \delta^* = \underset{1\le i\le n}{\text{med}}(\delta_i). \tag{4}$$

The parameter c describes the number of deviations from the central value to consider and is typically chosen between 2 and 3. Next section describes how the identified shape dissimilarities are taken into account to derive a more robust and geometrically meaningful alignment.

2.2 Iterative Displacement of Influential Points

The aim of the proposed algorithm is to derive an intermediate template with an improved distribution of landmarks residuals. It will be subsequently used as a link between the source and destination shapes to enable robust alignment. The intermediate template vector is denoted as $\hat{\mathbf{x}}$ (its inter-landmark-distances as $\hat{d}_{ij}$) and it is initialized with the source shape vector $\mathbf{x}^{(s)}$. To obtain $\hat{\mathbf{x}}$, each influential point $p_k \in A$ is displaced with the aim to minimize the associated large residual by approaching the invariant properties of $\mathbf{x}^{(d)}$. To this end, a displacement vector $d\hat{\mathbf{x}}_k$ is calculated such that it minimizes the sum of the associated inter-landmark differences, *i.e.*,

$$d\hat{\mathbf{x}}_k = \underset{d\hat{\mathbf{x}}_k}{\arg\min} \sum_{j\in B} (\hat{d}_{kj}(\hat{\mathbf{x}}_k + d\hat{\mathbf{x}}_k) - d_{kj}^{(d)})^2 \tag{5}$$

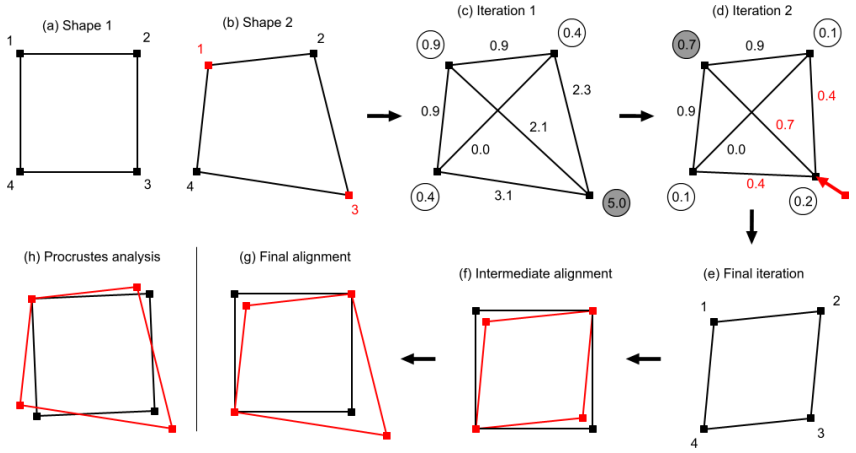

Fig. 1. Toy problem illustrating the main stages involved in the proposed technique. (a) and (b) show two quadrilaterals with differences at landmark 1 and 3. The calculated inter-landmark differences (see edges) and the associated landmark dissimilarity measures (Eq. (3), see circled) are displayed in (c) for iteration 1. The landmark 3 is identified as an influential point and displaced as shown in (d). It can be noticed how the associated inter-landmark discrepancies are decreased. At iteration 2 (d), the landmark 1 becomes an influential point and the algorithm continues until the intermediate template is obtained in (e). It can be seen how the transformation from (c) to (e) allows a balanced intermediate Procrustes alignment with the destination shape (f). The final result in (g) demonstrates good identification of the expected residuals. The Procrustes analysis alone in (h), however, introduces errors at all landmarks.

where B denotes the set of non-influential landmarks in the shape (*i.e.*, all landmarks in the shape minus A). By differentiation of (5), it can be easily shown that an improved $d\hat{\mathbf{x}}_k$ can be calculated at time $t+1$ based on the following formulae:

$$d\hat{\mathbf{x}}_k(t+1) = \alpha_k \sum_{j \in S} (\hat{d}_{kj}(t) - d_{kj}^{(d)}) \frac{(\hat{\mathbf{x}}_k(t) - \hat{\mathbf{x}}_j)}{\hat{d}_{kj}(t)}. \tag{6}$$

The parameter α_k is the optimal displacement step which can be found through simple line minimization. It is worth noting that $d\hat{\mathbf{x}}_k$ corresponds to a weighted sum of the unit vectors between $\hat{\mathbf{x}}_k$ and each non-influential point in B, where the weights $\hat{d}_{kj} - d_{kj}^{(d)}$ promote displacements in the directions corresponding to large inter-landmark discrepancies. The vector $d\hat{\mathbf{x}}_k$ is typically obtained after a number of successive displacements following Eq. (6). The inter-landmark distance matrices $\hat{\mathbf{D}}$ and $\mathbf{D}^{(d)}$ are subsequently updated, followed by a new round of influential point detection and displacement. This iterative approach is a key element of the proposed technique as it allows identifying both large and less significant shape differences. The most severe landmark residuals are typically detected during the initial iterations. After their correction, their effects are eliminated which facilitates the identification of less severe influential landmarks at subsequent iterations. The iterative procedure

then is repeated until no influential point remains, indicating that the shape differences between $\hat{\mathbf{x}}$ and $\mathbf{x}^{(d)}$ become normally distributed along all landmarks. Finally, a Procrustes alignment is carried out between the intermediate and destination shapes, followed by the application of the corresponding parameters to the original vector $\mathbf{x}^{(s)}$ for final alignment with $\mathbf{x}^{(d)}$.

It is worth mentioning that unlike existing techniques, the inter-point Procrustes has an interpretative power since it explicitly distinguishes between common structures and dissimilar regions in the shape. The proposed algorithm is now summarized in Table 1 and illustrated in the synthetic example of Fig. 1.

Table 1. Listing for the proposed alignment algorithm

1.	$\mathbf{x}^{(s)}$ and $\mathbf{x}^{(d)}$ are the input shape vectors. $\hat{\mathbf{x}}$ is the output intermediate vector initialized as $\hat{\mathbf{x}} = \mathbf{x}^{(s)}$.
2.	Calculate the inter-landmark distance matrices $\hat{\mathbf{D}}$ and $\mathbf{D}^{(d)}$.
3.	Calculate the median discrepancy values δ_i.
4.	Identify the set of influential landmarks A (Eq. (4)).
5.	If $A = \varnothing$ go to step (**8**).
6.	Displace the influential points in A (Eq. (6)).
7.	Go to step (**2**).
8.	Align $\hat{\mathbf{x}}$ and $\mathbf{x}^{(d)}$ using the standard Procrustes analysis.
9.	Apply the pose parameters from step **(8)** to the source shape $\mathbf{x}^{(s)}$.

3 Results

For numerical assessment, the robustness of the proposed technique is evaluated with respect to the severity of regional shape differences. To this end, a 3D liver dataset (Fig. 3) is used to synthetically create regional deformations, by randomly selecting and deforming a localized group of landmarks based on uniform noise. Varying percentages of deformed landmarks and amplitudes of deformation are simulated as shown in Fig. 2. Additionally, a perturbation of all landmarks is carried out using zero mean Gaussian noise. For comparison purposes, the standard Procrustes and a robust extension based on M-estimators [6] are implemented. It is evident from the results in Fig. 2 that the proposed technique outperforms existing Procrustes methods.

The improvement becomes particularly marked as the number of extreme residuals (a) and their amplitude increase (b). The robust Procrustes improves upon the least squares results up to a certain percentage of landmarks involved in the localized dissimilarity (around 20%). The proposed alignment, however, displays a higher breakdown point (close to 50%) and can handle large residuals as a result of the invariant influential point detection. Fig. 3 shows an example of regional shape deformation involving the left lobe of the liver (shown by the arrows). The influential points as detected by the proposed technique are displayed in dark shading in (c),

where it can be seen that the left lobe is correctly highlighted. This is a key feature of the proposed alignment which can be used as a quantitative as well as a visualization tool for shape interpretation.

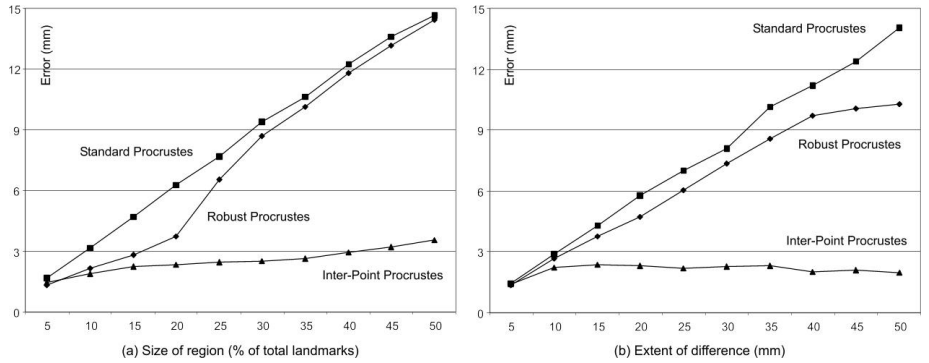

Fig. 2. Effects of the number of landmarks (a) and extent of localized deformation (b) on shape alignment by using the proposed algorithm and the techniques used for comparison. In (a), the amplitude is fixed to 30 mm, while in (b) the percentage of deformed landmarks equals 25%.

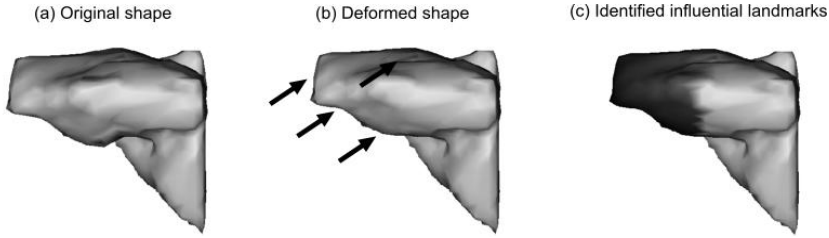

Fig. 3. Illustration of the performance of the proposed algorithm in explicit identification and visualization of regional shape differences

The proposed technique is then applied to a real dataset consisting of human carotid arteries. Such anatomical tree-like structures are very prone to large regional differences. In particular, existing research has shown that the geometry of the bifurcation is an important heamodynamic factor for the genesis and progression of atherosclerotic plaque. In this application, we have collected two classes of real carotid artery datasets. The first class contains 26 carotids with normal bifurcation geometry (example in Fig. 5(a)) and the second consists of three carotids with a genetic distortion of the external branch (example in Fig. 5(b)) as identified by the clinician (and referred to as wide-angle bifurcations). Both the standard and the inter-point Procrustes were then applied to the entire sample for shape discrimination and the results based on the first two modes of variation are plotted in Fig. 4. It can be seen that the separation between the two classes with the existing Procrustes is rather subtle, yet these shapes are significantly different as illustrated in Figs. 5(a) and (b). With the proposed technique, however, the class separation becomes pronounced.

This is because the proposed technique explicitly identifies the major regional differences (in this case the external branch), which are then taken into account during the intermediate alignment step. Unlike the method in [3], no supervision and user input is required to separate the three abnormal cases from the rest of the arteries.

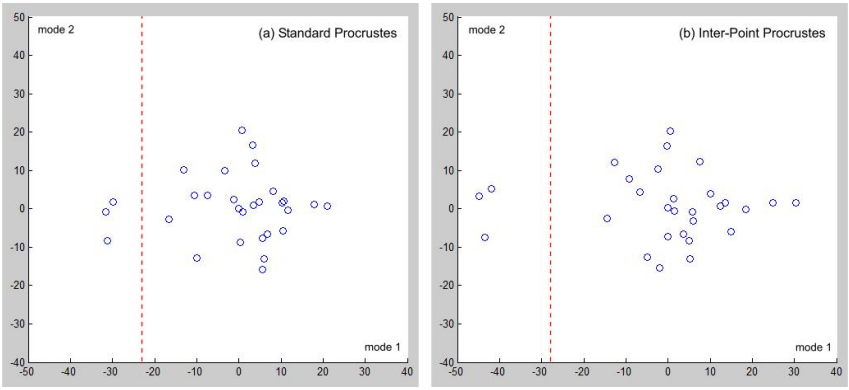

Fig. 4. Discrimination of the real carotid datasets by both the standard and proposed Procrustes

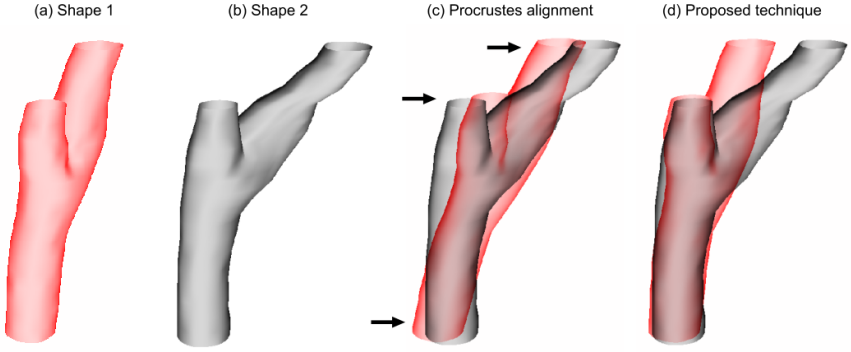

Fig. 5. Illustration of the strength of the proposed method for highlighting regional differences in tree-like structures. The carotid arteries in (a) and (b) differ significantly in their external branch, as detected by the proposed technique (d). The Procrustes analysis in (c), however, introduces alignment errors at various areas of the artery as shown by the arrows.

The strength of the proposed is further demonstrated in Fig. 5, where two carotids taken from the two classes are aligned with both the least-square Procrustes and the proposed method. Figs. 5(a) and 5(b) differ in various areas of the artery but with an evident large dissimilarity in the shape of their external branches (see Fig. 5(b)). In such a situation, the Procrustes analysis in Fig. 5(c) tends to distribute the residuals along the carotid, thus introducing alignment artifacts at the main branch and at the bifurcation as shown by the arrows. Although the gold standard alignment for real datasets is unknown a priori, it is evident that the proposed technique enables

improved fitting of the main and internal arteries, while the difference in the external artery is now fully highlighted. This demonstrates the benefit of the introduced technique to obtain anatomically meaningful results.

4 Conclusions

We have presented an inter-point Procrustes technique for robust shape alignment and interpretation. Unlike the standard method which minimizes a predefined matching criterion, the proposed approach is geometrically and biologically motivated: it explicitly identifies the common structures and the dissimilar regions in the shapes under investigation. This important information is taken into account during the alignment, which means the true shape differences can be highlighted in subsequent analysis. The validation shows that the technique can handle single-part (*e.g.*, liver) or multi-part (*e.g.*, tree-like structures) morphologies with a significant robustness to the severity of the regional differences. The results also suggest a potential interpretative value particularly for regional shape analysis and anatomical classification.

Acknowledgment. This work was partly funded by the Spanish Ministry of Science and Innovation (Grant TIN2009-14536-C02-01) and partly by the U.K. Engineering and Physical Sciences Research Council (Grant GR/T06735/0). Karim Lekadir was supported by a Juan de la Cierva fellowship from the Spanish Ministry of Science and Innovation.

References

1. Dryden, I.L., Mardia, K.V.: Statistical shape analysis. Wiley, New York (1998)
2. Cootes, T.F., et al.: Active shape models - Their training and application. Computer Vision and Image Understanding (CVIU) 61(1), 38–59 (1995)
3. Loog, M., de Bruijne, M.: Discriminative Shape Alignment. In: Prince, J.L., Pham, D.L., Myers, K.J. (eds.) IPMI 2009. LNCS, vol. 5636, pp. 459–466. Springer, Heidelberg (2009)
4. Suinesiaputra, A., et al.: Automated detection of regional wall motion abnormalities based on a statistical model applied to multislice short-axis cardiac MR images. IEEE Transactions on Medical Imaging 28(4), 595–607 (2009)
5. Dorst, L.: First order error propagation of the procrustes method for 3D attitude estimation. IEEE Transactions on Pattern Analysis and Machine Intelligence 27, 221–230 (2005)
6. Verboon, P., Heiser, W.J.: Resistant orthogonal Procrustes analysis. Journal of Classification 9, 237–256 (1992)
7. Larsen, R.: L1 generalized Procrustes 2D shape alignment. Journal of Mathematical Imaging and Vision 31, 189–194 (2008)
8. Huber, P.J.: Robust statistics. Wiley, New York (1981)